IUST
Iran University of Science and Technology

Iranian Journal of Electrical and Electronic Engineering

Journal Homepage: ijeee.iust.ac.ir

Research Paper

Two-Stage Islanding Detection Method via High Frequency Impedance and Harmonic Distortion Evaluation in Multi-DG Networks

M. Mohiti*, S. Sabzevari**, P. Siano***(C.A.)

Abstract: Islanding detection is essential for reliable and safe operation of systems with distributed generations (DG). In systems with multiple DGs, the interaction between DGs can make the islanding detection process more challenging. To address this concern, this paper proposes a two-stage islanding detection method for power systems equipped with multiple-DGs through estimation of high frequency impedance (Z_f) and determination of the total harmonic distortion (THD). The impedances of the DGs are estimated at distinct frequencies to avoid interval overlaps. The concept of different frequency bands makes the proposed method applicable to multiple DG systems. To evaluate the effectiveness of the proposed method, a test system with multiple DGs is simulated through several case studies in PSCAD/EMTDC. The simulation results demonstrate the accuracy of the proposed islanding detection method in both single and multi-DG systems. It is also shown that the proposed method remains robust under different operating conditions and events.

Keywords: Islanding Detection, Decentralized Method, High Frequency, Impedance Estimation, Multi-DG.

1 Introduction

IN recent years with the increasing demand and price of electricity, integration of DGs in power systems has increased significantly due to their environmental benefits. However, penetration of DGs in the power system brings challenges such as islanding. Islanding is a situation in which the DG continues to supply power to its loads following an interruption that suspends power supply from the main network. Unintentional islanding can cause potential threats to the system personnel, power quality and reliability of customer service [1].The current utility practice and standards require that the islanding event be detected as fast as possible. However, the trends in the integration of distributed energy resources indicate that the islanded operation will be accepted in the future [2].

Rich literature has been presented on islanding detection methods. Generally, islanding detection methods are classified into two categories: 1) remote detection methods 2) local detection methods. Remote methods are built upon telecommunication infrastructure and use procedures such as supervisory control and data acquisition. The communication system based methods increase system investment cost [3, 4]. The local methods are further divided into passive and active methods.

Passive methods measure system parameters such as voltage, frequency and total harmonic distortion at the point of common coupling [5]. If the measured parameters exceed the specified thresholds, the situation is declared as islanding. The main disadvantage of passive methods is their large non-detection zone (NDZ). NDZs are the loading conditions in which the detection method may fail to detect islanding. This drawback becomes more challenging when the power mismatch (between the DG output and load demand) is zero. In this case the variation of system variables are negligible and islanding may not be detected. Many passive methods such as: over/under voltage, over/under

Iranian Journal of Electrical and Electronic Engineering, 2021.
Paper first received 30 July 2020, revised 15 January 2021, and accepted 18 January 2021.
* The author is with the Department of Electrical Engineering, Yazd University, Yazd, Iran.
E-mail: maryammohiti@gmail.com.
** The author is with the Department of Electrical and Computer Engineering, Semnan University, Semnan, Iran.
E-mail: san.sabzevari@gmail.com.
*** The author is with the Department of Management & Innovation Systems, University of Salerno, Salerno, Italy.
E-mail: psiano@unisa.it.
Corresponding Author: P. Siano.
https://doi.org/10.22068/IJEEE.17.3.1945

frequency [6], and total harmonic distortion (THD) have been proposed in the literature [7]. Reference [8] proposes a feedback based islanding detection method for one-cycle-controlled single-phase inverters. In the method introduced in [9] the derivative of the equivalent resistance seen from synchronous generators' terminal with respect to the angular frequency are extracted as the islanding index. In [10] a multi criteria passive islanding detection algorithm has been used to increase the reliability of the method. Authors of [11] present a passive islanding detection technique based on modal transformation of voltage signals and derive islanding detection factor from the extracted data.

Active methods inject a periodic or transient perturbation into the system and islanding is detected through evaluation of the system response. To account for power quality concerns, the injected disturbance should be kept as small as possible. The active methods presented in [12-14] vary a microgrid parameter such as voltage, phase, or frequency and evaluate the system response. Slip mode frequency shifting and active frequency drift methods are in the aforementioned group [15]. In some cases this manipulation of the microgrid variables could lead to its instability. In [16] a reference signal generator is integrated in a multi-level inverter of a PV system. This reference signal is synchronized with the utility grid signal and islanding is detected if the two signals are not in phase. The method presented in [17] estimates the grid impedance at the injected frequency. The main inconvenience of active methods is that they reduce the power quality of the system. In systems with multiple DGs, interferences may occur among DGs which may lead to failure of both islanding detection system and stability. In [18, 19], a master slave scenario is applied to avoid this interaction. The master inverter continuously injects a high frequency current into the DG control loop and islanding is detected by measuring the system impedance. In this method slave inverters should detect the signal injected by the master and adopt their control mode. One drawback of this method is that the measured impedance is the system impedance and inverters which are far from the master may not receive the injected signal. In [20], a high frequency transient signal injection based islanding detection method is proposed. In this paper the injection source is centralized at the point of common coupling and the impedance measured from the PCC is used for islanding detection. Although a centralized source for injection can have many advantages such as avoiding the interferences however, since in large systems the disturbance is far apart of some DGs and the variation of the measured impedance may not be large enough to be distinguished. Moreover, when the islanding detection unit is not placed in proximity of DGs, a communication based infrastructure is needed to inform the DGs to adopt their operation mode to the new situation.

Hybrid methods apply both passive and active methods to detect islanding. Therefore, they take advantages of both passive and active methods. In hybrid methods the active method is triggered by the passive method. In the literature different hybrid methods have been presented [21]. In [22] a hybrid islanding method is introduced in which voltage unbalance and total harmonic distortion are used to trigger the active method. In the active method bilateral reactive power variation is measured. In [23] optimized Sandia frequency shift is used as the passive method and rate of change of frequency relay is applied as the active method. Reference [24] presents a hybrid islanding detection method, through detection of voltage unbalance and impedance estimation. In multi-DG systems interaction between injected signals can occur, therefore the islanding detection method should be able to detect islanding for each DG independently of its location. Many islanding detection methods have been presented in literature but they have not considered their application to multi-DG systems. Reference [25] proposes an islanding technique suitable for multiple mini-hydro DG units. In this paper islanding is detected by measurement of the reactive power change. In [18] a centralized injection is used to avoid interaction between DGs and estimation of all DGs impedances are done at the same frequency. Hybrid methods in addition of not degrading the power quality have zero non detection zones.

In this paper, a hybrid islanding detection method for multiple-DG systems which is based on a combination of the high frequency impedance (Z_f) estimation and the total harmonic distortion (THD) measurement, is proposed. Average THD is used to trigger the perturbations detection signal in the DGs control loop. In practice, average THD and the impedance estimation has been used in islanding detection algorithms [10, 18]. These methods have not been adopted to the multiple DG systems islanding detection. In the proposed method of this work a "separation interval" is introduced in which the DG injection signals are perturbed at distinct frequencies and the related Z_f for every DG is estimated. The main contributions of this paper are listed in the following:

- The proposed method has the capability to detect islanding for every DG locally and independently. Therefore, it can be implemented into the multiple-DG systems.
- Due to application of a decentralized injection and the separate frequency bands, the proposed hybrid method can be implemented into a power system without any need to have an extra communication infrastructure.
- The proposed method is immune against the other power system ordinary transient events such as: the start-up of induction motors, the capacitor switching and the occurrence of faults.
- Since in the proposed method, each DG detects the

islanding individually, the detection process is fast, i.e. it will be finished within 1 s. Therefore, it is within the acceptable limits of IEEE 1547 [1] islanding detection time frame.

2 Proposed Multi-DG Islanding Detection Method

A schematic diagram of a multi-DG test system is depicted in Fig. 1. DGs are connected to the point of common coupling. Test conditions are defined according to UL1741 [2]. In this paper a hybrid islanding detection method for multi-DG systems is presented in which the two-stage total harmonic distortion evaluation and the high frequency impedance measurement are employed to detect the islanding.

2.1 Voltage Source Converter Control System

The Voltage Source Converter (VSC) control block diagram is illustrated in Fig. 2. The dq-frame current control method is adopted to control the VSC power [26]. As can be seen the feedback signals (I_d, I_q) and feedfoward signals (V_d, V_q) are provided by abc/dq transformation of the output voltage and current of VSC. The angle of the abc/dq transformation (θ) is synchronized with the grid frequency by a PLL to ensure the quadrate output voltage (V_q) is forced to zero. Therefore, the real and reactive power of the VSC are proportional to I_d and I_q respectively [27]. It should be mentioned that gating signals for the VSC are produced by Sinusoidal Pulse width modulation (SPWM).

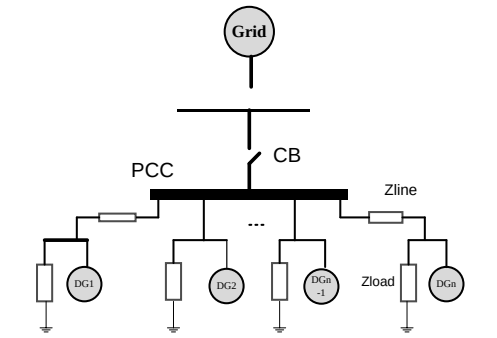

Fig. 1 Schematic diagram of the multi-DG system.

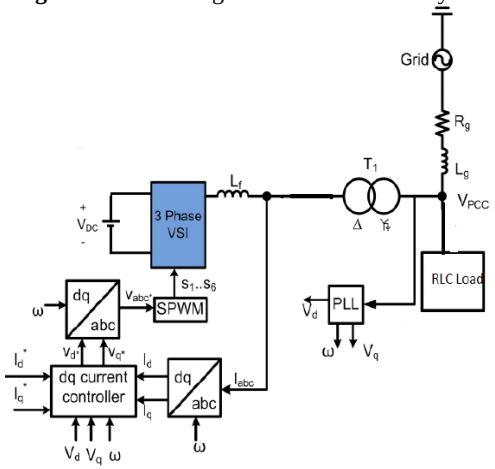

Fig. 2 Control system of VSC.

2.2 Principle of THD Measurement

When islanding happens in the network, the loading conditions and the network configuration will be changed. Therefore, especially in a system with converter based DGs, the THD at the DGs terminal will vary [10] .The total harmonic current distortion is determined as follows:

$$THD_t = \frac{\sqrt{\sum_{h=2}^{H} I_h^2}}{I_1} \quad (1)$$

Where, I_h is the rms of harmonic current h, I_1 the rms of the fundamental current, H is the expected number of harmonics and t is the monitoring instant. The average of THD_t is determined by (2). It is used to monitor its variations over time.

$$THD_{avg} = \frac{1}{N}\sum_{i=0}^{N-1} THD_{t-i} \quad (2)$$

Where, N is the number of samples in one cycle. In [10], THD is presented as a monitoring parameter to detect islanding operation, however it is discussed that it may not be reliable in distinguishing islanding from other network disturbances. In the proposed method a 10% threshold for THD_{avg} is set. THD_{avg} above 10% are suspicious of islanding and should be further investigated. To minimize the drawbacks of THD based islanding detection method, an active method is introduced and incorporated. Therefore, the THD is used to trigger the active method and avoid mal-operation due to ordinary transient events in the power system.

2.3 Principle of High Frequency Impedance Estimation

In Fig. 3, a schematic diagram of a multi-DG system equivalent circuit is shown. As it can be seen in this

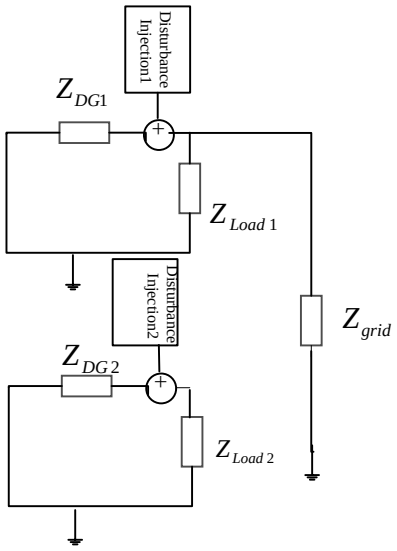

Fig. 3 Schematic diagram of a double-DG micro-grid system equivalent circuit.

figure, a perturbation is injected into each DG. In impedance estimation based islanding detection methods, usually the variations of the estimated impedance at the PCC is determined. The proposed method estimates impedance at DGs' terminal.

Fig. 4 illustrates the impedance estimation method in more details. As it can be seen a three phase sinusoidal voltage signal ($v_{abc,f}$) is injected into the DGs' inverter reference voltage injection point as a disturbance. The estimated impedance is calculated using (3):

$$Z_{fi} = \frac{V_{fi}}{I_{fi}} \tag{3}$$

where, Z_{fi} is the estimated impedance, V_{fi} and I_{fi} are the measured voltage and current at the terminal of the DG, respectively. In the impedance estimator block, the voltage and current at the DG's terminal are measured and a band-pass filter is used to isolate the high frequency components. Furthermore, a band stop filter is used in the DG current regulator to avoid interaction between the high frequency component and the fundamental signal.

This active method is applied into all DGs. The only difference between the active method implemented for different DGs of the system is that the injected signal frequency is distinct for every DG. The impedances are estimated at the frequency of the injected voltage signal and the band-stop and band-pass filters of Fig. 3 are tuned for the aforementioned frequency. Since the injected signal into each DG has a distinct frequency, therefore the different DGs have different frequency bands used for the impedance estimation block. To ensure that all the DGs have distinct frequency bandwidths; Eq. (4) is used to determine the injected voltage frequency for each DG.

$$f_i = 2nf + (-1)^n \times 10, \qquad n \geq 2 \tag{4}$$

where, f is the system frequency, f_i is the frequency of the injected signal at DG_i. The injected signals' frequencies should be chosen so that a gap is allowed between them and from the power system frequency harmonics. Therefore, according to (4) the injected signals' frequencies are chosen within a 10 Hz bandwidth from the even harmonics of the fundamental frequency. This is due to the fact that in DGs' inverter, the gating signals for the switches are produced by sinusoidal pulse width modulation technique (SPWM) and in this method even harmonics are eliminated. Therefore, usually there is no even harmonic in their terminal voltage or current signals. Furthermore, since the proposed method estimates the impedance of the DGs at the injected signal frequencies and every DG has a distinct frequency bandwidth, the proposed method is implemented into the time domain. And, therefore the frequency domain analysis is not necessary. To avoid the side effects of phase voltage unbalances, the average equivalent impedance of the three phases is employed as shown in (5) and used for islanding detection:

$$Z_{DGi} = \frac{Z_{ai} + Z_{bi} + Z_{ci}}{3} \tag{5}$$

where, Z_{ai}, Z_{bi}, and Z_{ci} are the estimated equivalent impedances of phases a, b and c of the *i*-th DG at frequency of f_i, respectively. It should be mentioned in order to avoid malfunction the steady state value of Z_{DGij} is used for islanding detection. Therefore, after a 0.2 s delay in which the transient is damped, Z_{DGi}^{avg} is calculated according to (6) for 0.2 s time interval. This value (Z_{DGi}^{avg}) is used to detect the islanding status.

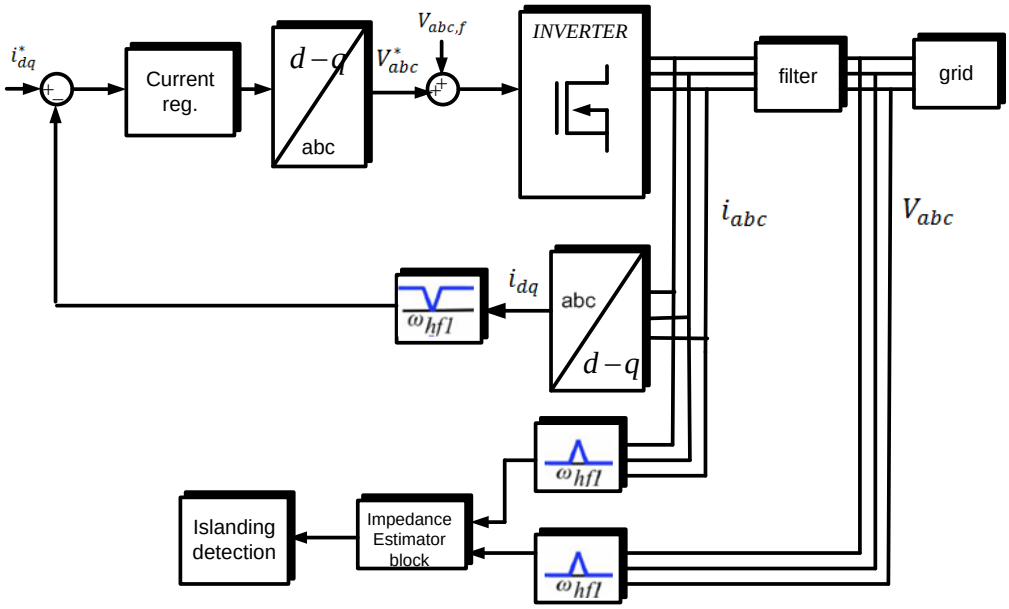

Fig. 4 Active islanding detection method implemented into a DG control loop.

$$Z_{DGi}^{avg} = \frac{1}{N}\sum_{k=0}^{N-1} Z_{DGi(t-k)} \quad (6)$$

where N is the number of samples in one cycle. Note that Z_{DGi}^{avg} is estimated after the active method is triggered, therefore, the 0.2 s delay starts after the trigger signal is sent. Furthermore, to evaluate the variation of Z_{DGi}^{avg} according to (7) the relative percent error of Z_{DGi}^{avg} is compared with a threshold.

$$RE = \frac{Z_{DGi}^{avg-AI} - Z_{DGi}^{avg-BI}}{Z_{DGi}^{avg-BI}} \times 100 \quad (7)$$

where Z_{DGi}^{avg-AI} and Z_{DGi}^{avg-BI} are the average steady state high frequency impedance of DG_i before and after islanding event, respectively.

2.4 Injected Signal Magnitude and Frequency

The magnitude of injected signal should be selected in such a way not to violate the power quality requirements of the power system. The signal magnitude should be large enough to make the detection possible, while the power quality is maintained in the permissible range. Connection standards [1] limit the voltage and current THD to 5%. In the proposed method the magnitude of the injected voltage is 5 V. The voltage THD before and after signal injection is 0.5% and 0.97%, respectively which is in agreement with the above requirements. In selecting the frequency several issues need to be considered. In case a RLC filter is used as the output filter of the VSC, the resonant frequency of the filter should be calculated to avoid interaction with the injection frequency. Furthermore, the interaction of the injection frequency with the grid resonant frequency should be investigated too. In case the injection frequency of any of the DGs is near the grid resonance frequency, the injection frequency of that DG should be changed by choosing another "n" in (4).

3 Hybrid Method Implementation

The proposed method of this work employs the active and the passive methods to develop a hybrid algorithm as depicted in Fig. 5. THD is monitored at the terminal voltage, and if it is to fluctuate wildly, the injection procedure is activated and a voltage signal is injected; with the frequency determined by (4); to every DG. After a 0.2 s delay the impedance of all DGs under their injection frequency is estimated, and if the RE is more than 25%, it shows that DG_i is islanded.

4 Simulation Results

The sample multi-DG network of Fig. 6 is simulated in PSCAD/EMTDC in to validate the proposed method of this work. Each DG shown in Fig. 5 satisfies the test conditions of UL1741 standard. In this test system the DG are modeled by a VSC with a series RL filter. According to UL1741 the load is tuned at 60 Hz to provide unit power factor. The system main parameters are shown in Table I. The THD threshold is set to 10% and the frequency of the injected signal for the DGs is calculated by (4) which are 250 Hz and 350 Hz for DG_1 and DG_2, respectively. The estimated impedance (Z_{DGi}^{avg}) of DG_1 and DG_2 (Z_{f1} and Z_{f2}) at the injected signals' frequencies are determined and shown versus time in Fig. 5, respectively.

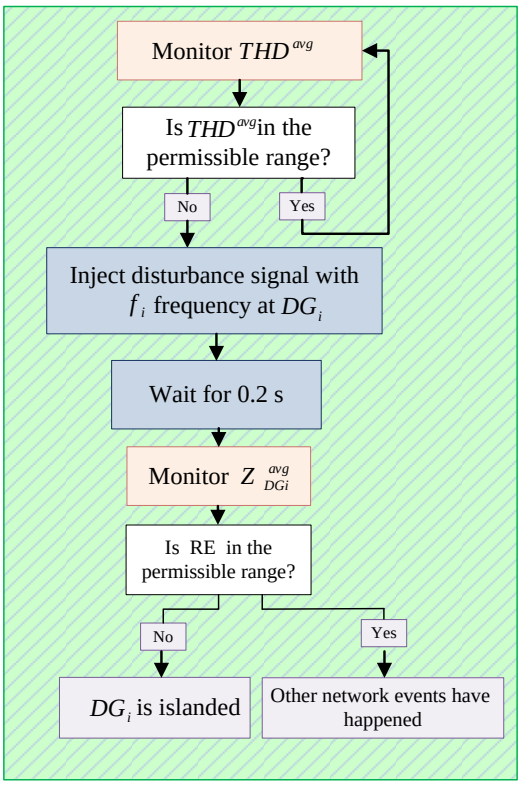

Fig. 5 Flow diagram of the proposed islanding detection method.

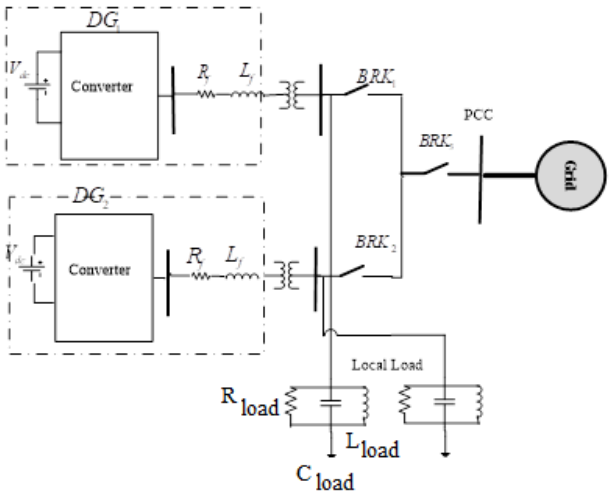

Fig. 6 Schematic diagram of the sample multi-DG network used for simulation of the method.

4.1 Case Study 1

In this case study the scenarios shown in Table 2 are simulated and the performance of the proposed method for a multiple DG system is studied. In scenario I, DG_1 is islanded and in scenario II all DGs are islanded. THD of DG_1 and DG_2 in scenario I are 11.86% and 13.67%, respectively. Consequently, a 250 Hz and 350 Hz signal is injected into DG_1 and DG_2 control loop, respectively. Z_{f1} and Z_{f2} are evaluated according to the proposed method and those are depicted, for this scenario, in Fig. 7. As can be observed values of RE for DG_1 and DG_2 are 71% and 12%. Therefore, islanding is only detected for DG_1. Fig. 8 shows estimated impedances for scenario II. In this scenario both DGs are islanded and THD_{avg} are above the permissible range (18.67% and 19.69%). Therefore, the signal injection division is triggered and Z_{f1} and Z_{f2} change significantly at t = 3.2 s. The RE values are 52% and 233% percent respectively. Subsequently, islanding is detected easily. These two scenarios show the effectiveness of the proposed method in detecting islanding in multiple DG systems.

4.2 Case Study 2

In this case study the following events happen: 1) at t = 1.7 s a load of (1 MW, 2 MVAr) is switched into the network at the PCC 2) at t = 2.2 s a 3 MVAr capacitor is switched into the network 3) at t = 3.2 s both DGs are islanded. Table 3 shows THD_{avg} of $DG_{1,2}$. As can be seen THD_{avg} of DG_1, exceeds its threshold (10%) for capacitor switching (t = 2.2 s) and islanding (t = 3.2 s) events. THD_{avg} of DG_2 exceeds permissible range only for islanding (t = 3.2 s) This is due to the fact that the capacitor and load switch are at DG_1's terminal and has less influence on DG_2. In the events which THD_{avg} exceed the permissible range the active method is triggered and the signals are injected to the DGs. Figs. 9 and 10 show variations of Z_{f1} and Z_{f2} over time, respectively. As it can be seen in Z_{f1} since injection is done for capacitor switching and islanding, the impedances experience a transient however, returns to the original value in a very short time, while under islanding event the impedance variations are high and the steady state condition which is significantly different and lead to a RE of 27% . Therefore, islanding is detected for DG_1. As mentioned THD_{avg} of DG_2 does not exceed threshold and no injection occurred under load or capacitor switching, Z_{f2} does not experience any variation under these events however, the islanding can be detected easily (through the THD change and consequently significant change in its impedance) which shows the credibility of the proposed method in multi-DG systems.

Table 1 Main parameters of the sample multi-DG network.

Parameters	Value
V_{dc}	6000 [V]
P	2.5 [MW]
L_f	0.0003 [H]
R_f	0.0015 [Ω]
Rload	76 [Ω]
Lload	0.1117 [H]
Cload	62.87[μF]

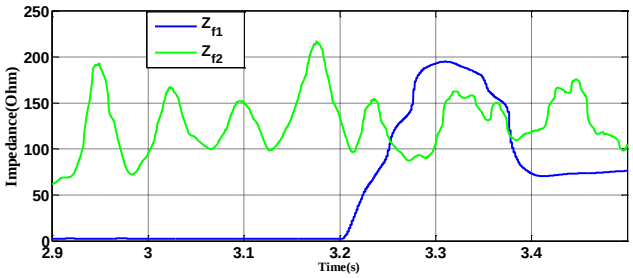

Fig. 7 Time variation of DGs' Impedances, as determined for scenario 1 of case study 1.

Table 2 Simulated scenarios in case study 1.

Scenario	Breaker switched	DGs islanded	Injected frequency
I	CB_1	DG_1	250 Hz
II	CB_2	DG_1, DG_2	350 Hz

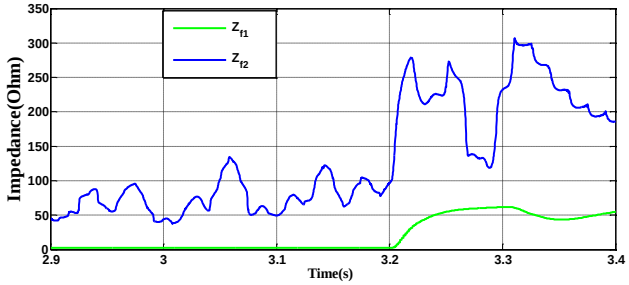

Fig. 8 Time variation of DGs' Impedances, as determined for scenario 2 of case study 1.

Table 3 THD_{avg} of DGs in case study 2.

Event	DG_1	DG_2
Load switching	%5.98	% 4.8
Capacitor switching	%11.2	%5.48
Islanding	%11.7	%17.75

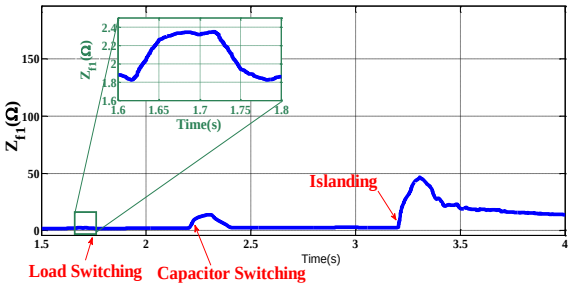

Fig. 9 Time variation of DG_1 Impedance, determined during case study 2.

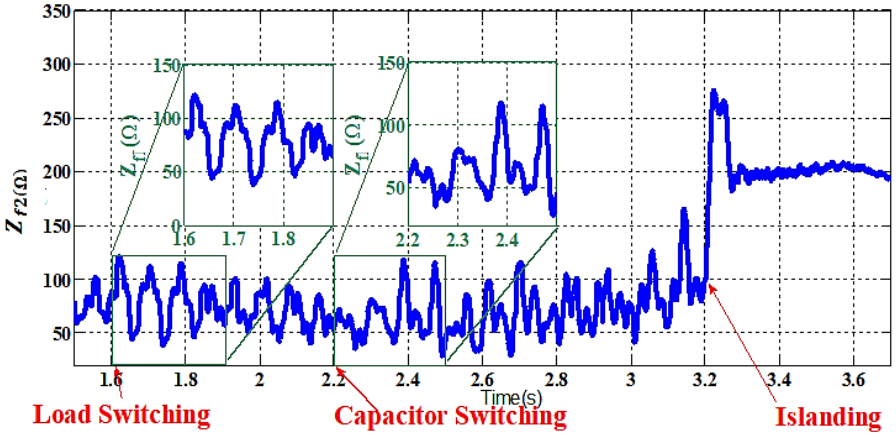

Fig. 10 Time variation of DG_2 Impedance, determined during case study 2.

Table 5 THD_{avg} of DGs in case study 3.

Event	DG_1	DG_2
Single phase fault	10.16%	7.37%
Two phase fault	13.88%	8.56%
Three phase fault	13.07%	21.02%
Islanding	20.79%	24.16%

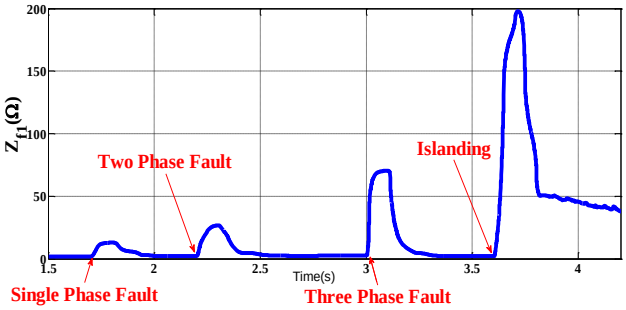

Fig. 11 Time variation of DG_1 impedance, determined during case study 3.

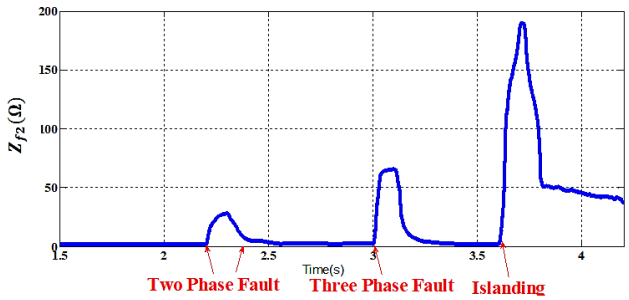

Fig. 12 Time variation of DG_2 impedance, determined during case study 3.

Table 6 Parameters of induction motor.

Parameter	Value
Rated power	11 MVA
Stator reactance	0.046 pu
Stator resistance	0.066 pu
First cage resistance	0.298 pu
Second cage resistance	0.018 pu

Table 7 THD_{avg} of DGs in case study 4.

Event	DG_1	DG_2
Non-linear load switching	10.46%	6.87%
Islanding	37.57%	30.8%

4.3 Case Study 3

In this case study the sequence of the events are 1) at $t = 1.7$ s a single phase fault 2) $t = 2.2$ s a two phase fault 3) at $t = 3$ s a three phase fault 4) at $t = 3.7$ s both DGs are islanded. Table 5 shows THD_{avg} of $DG_{1,2}$. The faults are located at the PCC. For DG_1 according to Table 5 all events result in an override in THD_{avg} therefore, signal injection is performed and as shown in Fig. 11, Z_{f1} varies at these events. As it can be seen for the faults the steady state value of the estimated impedance does not change considerably and the RE for the single, two phase, three phase faults 4.5%, 6.1%, and 9.4%, respectively. However, RE for islanding is 76%. Therefore, islanded is detected easily. In Fig. 12, THD_{avg} of DG_2 exceed the permissible range for all events except than single phase fault therefore, the signal injection is triggered for the three latter events and as a result Z_{f2} experiences variation for these events and RE for two phase, three phase faults, and islanding are 11% , 14%, and, 66%, respectively. Consequently, the islanding can also be distinguished from system faults with the proposed method and each DG can detect islanding autonomously.

4.4 Case Study 4

In this case study a nonlinear load is switched at $t = 2.2$ s and the DGs are islanded at $t = 3$ s. The nonlinear load is a squirrel cage induction motor with parameters presented in Table 6. According to Table 7 for DG_1 in both events THD_{avg} exceeds 10% and a

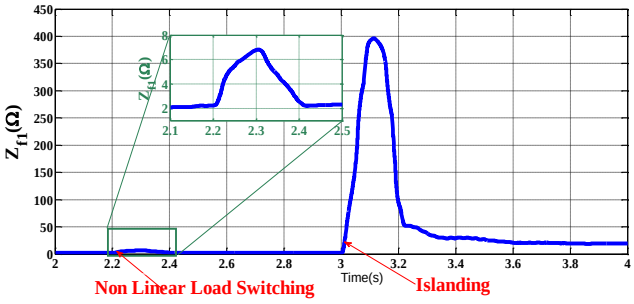

Fig. 13 Time variation of DG_1 impedance, determined during case study 4.

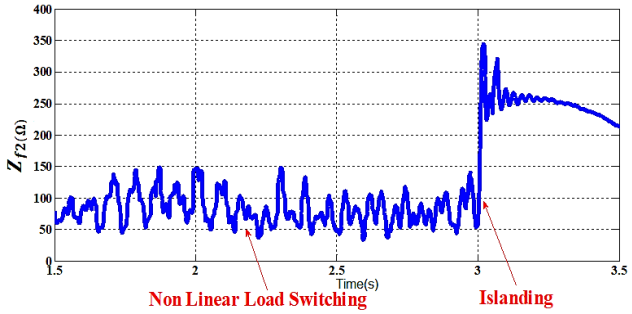

Fig. 14 Time variation of DG_2 impedance, determined during case study 4.

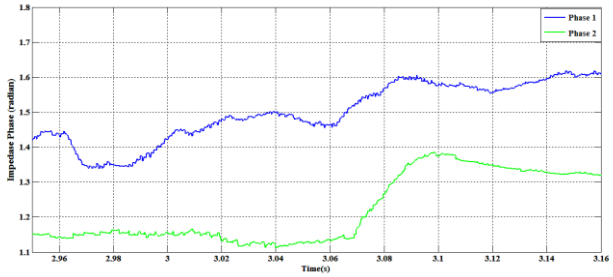

Fig. 15 Time variation of $DG_{1,2}$ phase of Impedance, determined during case study 5.

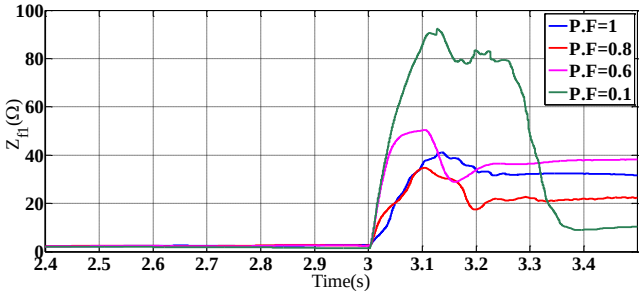

Fig. 16 Time variation of DG_2 impedance under different power factors.

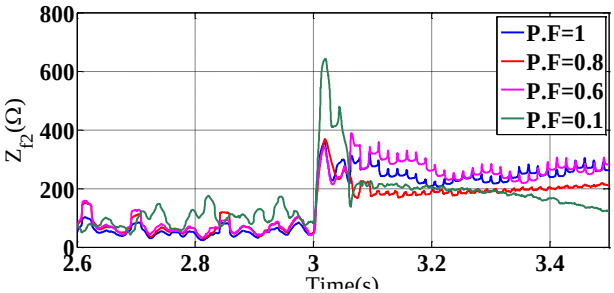

Fig. 17 Sensitivity analysis of DG_2 Impedance under different power factors.

250 Hz signal is injected to DG_1. As it can be seen in Fig. 13, Z_{f1} varies slightly for load switching and results in a RE of 0.1%, while Re for islanding is 47% for islanding therefore, it can be differentiated from nonlinear load switching easily. As it can be seen in Fig. 13 THD_{avg} of DG_2 exceeds the permissible range only under islanding process while, no perturbation happens under load switching event. Since Z_{f2} has no variation under load switching, by this method only islanding is detected at t = 3 s as seen Fig. 14.

4.5 Case Study 5

As mentioned earlier, the previous case studies are simulated on UL1741 anti-islanding test system and the magnitude of impedance is used to detect islanding. However, in networks where the high amount of capacity is used for reactive power compensation, the magnitude of the high frequency impedance before and after islanding may be close. In these cases monitoring the phase of the high frequency impedance is beneficial and the change of the phase of the system can be used to enhance the reliability of the method. It should be mentioned the phase of the impedance may increase or decrease depending on the current power factor and characteristic of the gird. To investigate this, a condition is considered where the grid exchanges 6 Mvar reactive power with the DGs network and the phase of the impedance in case study 5 is investigated. In this case islanding occurs at t = 3 s. As can be seen in Fig. 15 the phase of the high frequency impedance changes significantly and it can be used as a supplementary indicator for islanding detection.

5 Sensitivity Analysis

In this section the sensitivity of the proposed method to different system parameters is analyzed. The range of variation of the parameters under study are chosen such that the system remains stable before and after islanding (at t = 3 s). It should be mentioned that under all simulations, THD exceeds the permissible threshold. The interested factors are investigated in the following subsections.

5.1 Power Factor

The power factor of the DGs can affect Z_{f1} and Z_{f2}. When using the islanding detection methods under non-detection zones, islanding of a DG under a unit power factor may not be detected. In this section the power factors of DG_1 and DG_2 are varied from 0.1 to 1. As it can be seen in Figs. 16 and 17 even having a unit power factor (worst case) the islanding can be detected.

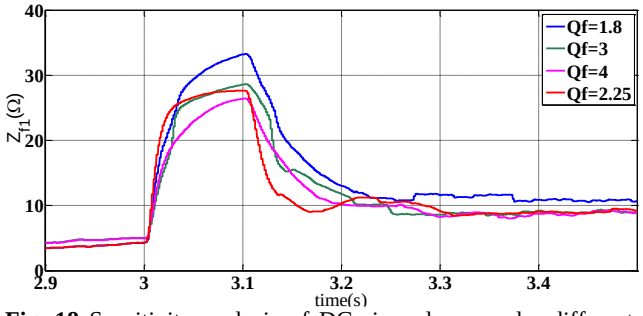

Fig. 18 Sensitivity analysis of DG_1 impedance under different quality factors.

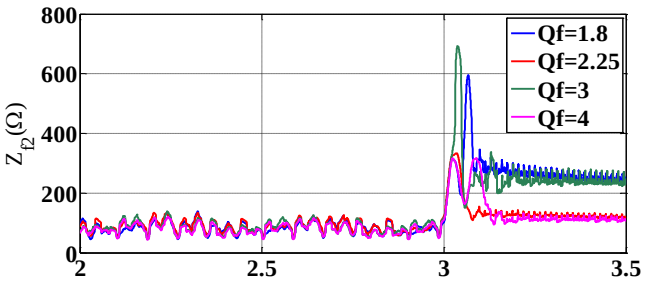

Fig. 19 Sensitivity analysis of DG_2 impedance under different quality factors (X_g/R_g = 2.1).

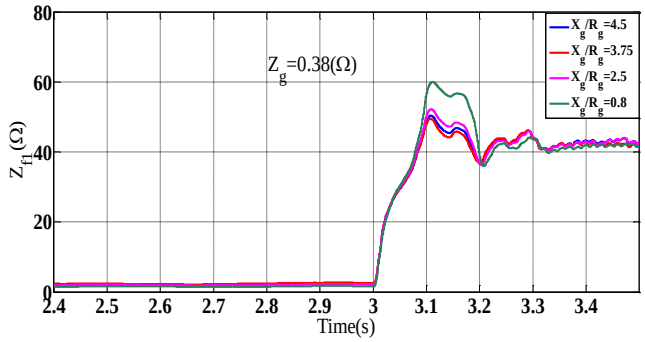

Fig. 20 Sensitivity analysis of DG_1 impedance under different X_g/R_g ratios.

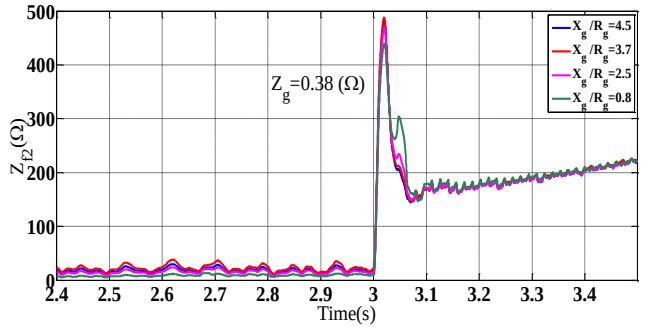

Fig. 21 Sensitivity analysis of DG_2 impedance under different X_g/R_g ratios.

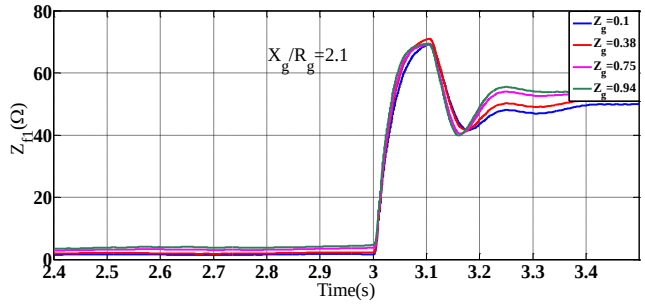

Fig. 22 Sensitivity analysis of DG_1 impedance under different Z_g values.

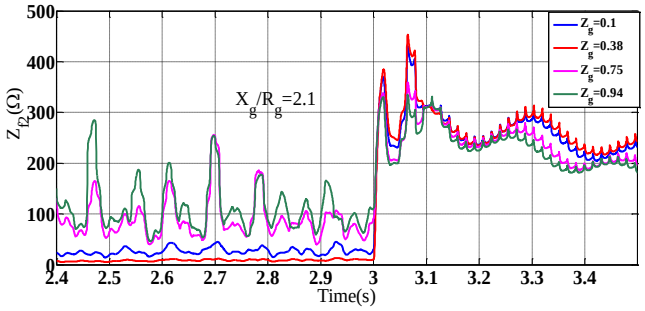

Fig. 23 Sensitivity analysis of DG_2 impedance under different Z_g values.

5.2 Load Parameters

In this section the variation of load quality factor (Q_f) is studied while others parameters are set constant. In Figs. 18 and 19, Q_f is varied from 1.8 to 2.25 and f_0 is set to 60Hz. As it can be seen with the variation of Q_f the transients of Z_{f1} and Z_{f2} change slightly. However, islanding condition can be detected regardless of the value of Q_f.

5.3 Grid Parameters

The grid parameters such as impedance magnitude (Z_g) and X_g/R_g ratio can affect the impedance. A weak grid is represented by a high impedance or X_g/R_g ratio. In Figs. 20 and 21 Z_g is kept constant while X_g/R_g is varied and Z_{f1} and Z_{f2} are depicted respectively. As can been seen the X_g/R_g ratio only effects the transient behaivour slighty and islanding can be detected in all cases. Figs. 22 and 23 corresponds to X_g/R_g = 2.1 and $Z_g \in [0.8, 0.94]$ and Z_{f1} and Z_{f2} illustrated, respectively. The results show that the proposed method can detect islanding event under both weak and strong grids conditions.

6 Conclusion

In this paper a hybrid islanding detection method for multi-DG systems is presented. Islanding is detected through application of a two-stage islanding detection method in which the average THD is employed to trigger high frequency impedance estimation. The proposed method uses a band separation concept to avoid interaction between different DGs in multi-DG systems. This feature allows the proposed method to be used in microgrids and in multi-DG power systems. Moreover, injection signal are perturbed in a decentralized manner. Therefore, islanding can be

detected locally. The simulations are performed on a multi-DG system according to IEEE 1547 standard. The results show that the proposed method can detect the islanding occurrence effectively (in both single and multiple DG systems). Meanwhile, it is shown that this method is robust against the other system events.

References

[1] "IEEE standard for interconnecting distributed resources with electric power systems," *IEEE Std 1547-2003*, pp. 1–28, 2003.

[2] "Inverters, converters, and controllers for use in independent power systems," *No. UL STD 1741*, 2002.

[3] H. Laaksonen, "Advanced islanding detection functionality for future electricity distribution networks," *IEEE Transactions on Power Delivery*, Vol. 28, No. 4, pp. 2056–2064, 2013.

[4] C. Li, C. Cao, Y. Cao, Y. Kuang, L. Zeng, and B. Fang, "A review of islanding detection methods for microgrid," *Renewable and Sustainable Energy Reviews*, Vol. 35, pp. 211–220, 2014.

[5] S. Raza, H. Mokhlis, H. Arof, J. A. Laghari, and L. Wang, "Application of signal processing techniques for islanding detection of distributed generation in distribution network: A review," *Energy Conversion and Management*, Vol. 96, pp. 613–624, 2015.

[6] J. C. M. Vieira, W. Freitas, X. Wilsun, and A. Morelato, "Performance of frequency relays for distributed generation protection," *IEEE Transactions on Power Delivery*, Vol. 21, No. 3, pp. 1120–1127, 2006.

[7] A. M. Massoud, K. H. Ahmed, S. J. Finney, and B. W. Williams, "Harmonic distortion-based island detection technique for inverter-based distributed generation," *IET Renewable Power Generation*, Vol. 3, No. 4, pp. 493–507, 2009.

[8] V. R. Reddy and S. S. E, "A feedback-based passive islanding detection technique for one-cycle-controlled single-phase inverter used in photovoltaic systems," *IEEE Transactions on Industrial Electronics*, Vol. 67, No. 8, pp. 6541–6549, 2020.

[9] R. Bekhradian, M. Davarpanah, and M. Sanaye-Pasand, "Novel approach for secure islanding detection in synchronous generator based microgrids," *IEEE Transactions on Power Delivery*, Vol. 34, No. 2, pp. 457–466, 2019.

[10] J. Sung-Il and K. Kwang-Ho, "An islanding detection method for distributed generations using voltage unbalance and total harmonic distortion of current," *IEEE Transactions on Power Delivery*, Vol. 19, No. 2, pp. 745–752, 2004.

[11] Y. M. Makwana and B. R. Bhalja, "Experimental performance of an islanding detection scheme based on modal components," *IEEE Transactions on Smart Grid*, Vol. 10, No. 1, pp. 1025–1035, 2017.

[12] G. Hernandez-Gonzalez and R. Iravani, "Current injection for active islanding detection of electronically-interfaced distributed resources," *IEEE Transactions on Power Delivery*, Vol. 21, No. 3, pp. 1698–1705, 2006.

[13] M. A. Hosani, Z. Qu, and H. H. Zeineldin, "Development of dynamic estimators for islanding detection of inverter-based DG," *IEEE Transactions on Power Delivery*, Vol. 30, No. 1, pp. 428–436, 2015.

[14] A. Emadi and H. Afrakhte, "A reference current perturbation method for islanding detection of a multi-inverter system," *Electric Power Systems Research*, Vol. 132, pp. 47–55, 2016.

[15] M. Karimi, H. Mohamad, H. Mokhlis, and A. H. A. Bakar, "Under-frequency load shedding scheme for islanded distribution network connected with mini hydro," *International Journal of Electrical Power & Energy Systems*, Vol. 42, No. 1, pp. 127–138, 2012.

[16] K. M. Tsang and W. L. Chan, "Rapid islanding detection using multi-level inverter for grid-interactive PV system," *Energy Conversion and Management*, Vol. 77, pp. 278–286, 2014.

[17] L. Asiminoaei, R. Teodorescu, F. Blaabjerg, and U. Borup, "A new method of on-line grid impedance estimation for PV inverter," in *Nineteenth Annual IEEE Applied Power Electronics Conference and Exposition*, Vol. 3, pp. 1527–1533, 2004.

[18] D. Reigosa, F. Briz, C. B. Charro, P. Garcia, and J. M. Guerrero, "Active islanding detection using high-frequency signal injection," *IEEE Transactions on Industry Applications*, Vol. 48, No. 5, pp. 1588–1597, 2012.

[19] D. Reigosa, F. Briz, C. Blanco, P. García, and J. M. Guerrero, "Active islanding detection for multiple parallel- connected inverter-based distributed generators using high frequency signal injection," in *IEEE Energy Conversion Congress and Exposition (ECCE)*, pp. 2719–2726, 2012.

[20] K. Jia, H. Wei, T. Bi, D. W. P. Thomas, and M. Sumner, "An islanding detection method for multi-DG systems based on high-frequency impedance estimation," *IEEE Transactions on Sustainable Energy*, Vol. 8, No. 1, pp. 74–83, 2017.

[21] A. Hariri and M. O. Faruque, "Performing islanding detection in distribution networks with interconnected photovoltaic systems using a hybrid simulation tool," in *IEEE Power and Energy Society General Meeting (PESGM)*, pp. 1–5, 2016.

[22] G. Wang, F. Gao, J. Liu, Q. Li, and Y. Zhao, "Design consideration and performance analysis of a hybrid islanding detection method combining voltage unbalance/total harmonic distortion and bilateral reactive power variation," *CPSS Transactions on Power Electronics and Applications*, Vol. 5, No. 1, pp. 86–100, 2020.

[23] M. Khodaparastan, H. Vahedi, F. Khazaeli, and H. Oraee, "A novel hybrid islanding detection method for inverter-based DGs using SFS and ROCOF," *IEEE Transactions on Power Delivery*, Vol. 32, No. 5, pp. 2162–2170, 2017.

[24] M. Mohiti, Z. Mahmoodzadeh, and M. Vakilian, "A hybrid micro grid islanding detection method," in *13th International Conference on Environment and Electrical Engineering (EEEIC)*, pp. 342–347, 2013.

[25] J. A. Laghari, H. Mokhlis, A. H. A. Bakar, and M. Karimi, "A new islanding detection technique for multiple mini hydro based on rate of change of reactive power and load connecting strategy," *Energy Conversion and Management*, Vol. 76, pp. 215–224, 2013.

[26] H. Karimi, A. Yazdani, and R. Iravani, "Negative-sequence current injection for fast islanding detection of a distributed resource unit," *IEEE Transactions on Power Electronics*, Vol. 23, No. 1, pp. 298–307, 2008.

[27] A. Yazdani and R. Iravani, "A unified dynamic model and control for the voltage-sourced converter under unbalanced grid conditions," *IEEE Transactions on Power Delivery*, Vol. 21, No. 3, pp. 1620–1629, 2006.

M. Mohiti received the B.Sc. and M.Sc. degrees from Sharif University of Technology, Tehran, Iran, in 2011 and 2013, respectively, and the Ph.D. degree in Electrical Engineering from the University of Tehran, Tehran, Iran, 2019. Her research interest includes microgrids operation, control, and protection, AI aided power system control, power system resilience, and energy storages.

S. Sabzevari was born in 1988. She received the B.Sc. and M.Sc. degrees from Ferdowsi University of Mashhad, Mashhad, Iran, in 2010 and 2013, respectively, and the Ph.D. degree in control engineering from Malek Ashtar University of Technology, Tehran, Iran, 2020. She is currently university lecturer at Semnan University. Her research interest includes machine learning, neural network, nonlinear observer, attitude estimation, intelligent methods, modeling and simulation, robotics, renewable and sustainable energy, and control.

P. Siano (M'09–SM'14) received the M.Sc. degree in Electronic Engineering and the Ph.D. degree in information and Electrical Engineering from the University of Salerno, Salerno, Italy, in 2001 and 2006, respectively. He is a Professor and Scientific Director of the Smart Grids and Smart Cities Laboratory with the Department of Management & Innovation Systems, University of Salerno. His research activities are centered on demand response, on the integration of distributed energy resources in smart grids and on planning and management of power systems. He has co-authored more than 450 papers including more than 200 international journal papers that received more than 7000 citations with an H-index equal to 43. He has been the Chair of the IES TC on Smart Grids. He is Editor for the Power & Energy Society Section of IEEE Access, IEEE Transactions ON Industrial Informatics, IEEE Transactions on Industrial Electronics, Open Journal of the IEEE IES and of IET Renewable Power Generation.